



Tool remaining useful life prediction method based on LSTM under variable working conditions

Jing-Tao Zhou¹ · Xu Zhao¹ · Jing Gao¹

Received: 21 April 2019 / Accepted: 23 August 2019
© Springer-Verlag London Ltd., part of Springer Nature 2019

Abstract

Tool remaining useful life prediction is important to guarantee processing quality and efficient continuous production. Tool wear is directly related to the working conditions, showing a complex correlation and timing correlation, which makes it difficult to predict the tool remaining useful life under variable conditions. In this paper, we seek to overcome this challenge. First, we establish the unified representation of the working condition, then extract the wear characteristics from the processing signal. The extracted wear features and corresponding working conditions are combined into an input matrix for predicting tool wear. Based on this, the complex spatio-temporal relationship under variable working conditions is captured. Finally, using the unique advantages of the long short-term memory (LSTM) model to solve complex correlation and memory accumulation effects, the tool remaining useful life prediction model under variable working conditions is established. An experiment illustrates the effectiveness of the proposed method.

Keywords Variable working conditions · Tool remaining useful life prediction · Long short-term memory · Hilbert-Huang Transform

1 Introduction

Tool life is the sum of the cutting time from the moment a new tool is cut until the tool is scrapped. In a flexible production line, tool life prediction is important for workpiece surface quality and production efficiency. In the actual application scenario, tool life prediction in the mass production process has achieved some results [1]. For small batch and multi-variety production manufacturing conditions, unlike mass production, the working conditions of the tool change frequently and its life is often difficult to evaluate. Over-frequent tool change would increase the processing time,

while it is also difficult to guarantee the machining quality [2]. Furthermore, the common industrial practice of replacing or regrinding machining tools per conservative schedule is not cost-effective. Additionally, this method is not suitable for working conditions where the tool changes frequently [3]. Therefore, an effective tool remaining useful life prediction method is helpful for small batch and multi-variety production processes.

Generally, tool condition monitoring methods can be divided into direct and indirect methods. Direct methods measure the amount of tool wear using optical or image detection [4]. Although direct methods are intuitive and have high measurement accuracy, they are susceptible to environmental interference and require downtime detection. This is not flexible or mature enough in a growing dynamic manufacturing environment [1, 3, 5, 6]. Therefore, indirect methods have been widely used. Indirect methods establish a mapping relationship between the tool wear state and signal characteristics. Physical signals of the process are collected and intelligent algorithms are used to identify the tool wear state. Analysis of the current wear value provides the basis for tool maintenance [7].

At present, the tool wear prediction research based on indirect methods often requires the process parameters to be

✉ Jing-Tao Zhou
Zhoujt@nwpu.edu.cn

Xu Zhao
651928960@qq.com

Jing Gao
1094200428@qq.com

¹ Key Laboratory of Contemporary Design and Integrated Manufacturing Technology, Ministry of Education, Northwestern Polytechnical University, Xi'an, Shaanxi Province, China

unchanged (or assumed to be unchanged) during the process. Usually, one or more sets of different levels of main process parameters are given for an experiment. Then, the effect of working condition variables on the tool wear is evaluated. This method is not optimized for variable working conditions and its application is limited. Under variable working conditions, the process of using the tool is more complicated. We have summarized two points:

1. The interaction of multiple working conditions in space. This interaction refers to the relationship between the tool wear state and the working conditions within a certain time period. The same tool may process multiple workpieces in its life cycle. The working conditions, such as cutting parameters, workpiece materials and machine factors can vary. The relationship between different working conditions and wear is complicated and difficult to analyze. Tool wear is not caused by a specific factor, but by the interaction of multiple factors in multiple processes.
2. The correlation of the tool state in time. **Tool wear state is the cumulative result of the previous changes of the wear characteristics and operating conditions.** The different tool wear conditions in the previous period and the change of the machining behavior in the future time period directly affect the future wear state. The tool wear state of each process is affected by factors such as machine equipment, processing technology, processing environment, and raw materials. As the manufacturing process progresses, the tool wear state affected by the upstream process factors will propagate to the downstream process.

In order to predict the tool remaining useful life under variable working conditions with complex space-time relationship, this paper uses the LSTM network to model the wear process under variable working condition. LSTM [8] is a recurrent neural network (RNN) architecture. RNNs are “fuzzy” in the sense that they do not use exact templates from the training data to make predictions, but rather like other neural networks use their internal representation to perform a high-dimensional interpolation between training examples. Thus, such fuzzy prediction does not suffer from the curse of dimensionality and is therefore much better at modeling real-valued or multivariate data than exact matches [9]. We use LSTM for high-dimensional modeling, eliminating redundant working condition parameters and extracting appropriate working condition factors for feature learning. On the other hand, due to the correlation of the tool state in time, the future wear state is the cumulative result of the previous wear characteristics change and operating conditions change. **The LSTM model has a unique advantage in long-term memory information. Because of its special unit structure, it can handle long-distance dependence problems in sequence data and can solve gradient problems better.** Therefore, we try to use LSTM to

deal with the complex space-time relationship between working conditions and wear characteristics changes.

In summary, we have built a unique method framework to solve the problem of tool remaining useful life prediction under variable conditions.

First, collect the working conditions and machining signals during the cutting process. Second, extract the tool wear characteristics from the machining signal. Finally, the LSTM-based model is established to learn the complex space-time relationship of the tool wear process under variable working conditions. In turn, tool remaining useful life under current working condition is obtained.

The remaining sections are organized as follows: In the next section, we present the literature review on tool selection and transfer learning. After that, in Section 3, we generalize our approach and explain its principles. The experiment is described in Section 4. In Section 5, we show the experimental results and discuss the effectiveness of the method. Finally, concluding remarks are given in Section 6.

2 Related work

2.1 Tool wear monitoring method

At present, a large number of studies are carried out without changing the working conditions, concluding that the cutting speed, feed, and the depth of cut are the parameters with the most influence on tool wear process [10]. Also, many physical model methods or numerical (finite element) methods are being refined [11–15]. However, most of the above similar methods have limitations on wear assumptions. Karuppusamy et al. proposed a system to monitor tool wear by using the captured image of the cutting tool tip and using a linear regression model to calculate tool wear [16]. Daddona et al. proposed a method that uses images of the cutting tool's worn-zone to train the artificial neural network (ANN) and then to perform the DNA-based computing (DBC). It is demonstrated that the ANN can predict the degree of tool-wear from a set of tool-wear images processed under a given procedure whereas the DBC can identify the degree of similarity/dissimilar among the processed images [17]. Many researchers have conducted extensive research on tool condition monitoring [18–20] using different sensing functions (cutting force, spindle power, torque, acceleration, current and acoustic emission, etc.) to collect information for early detection. **These attempts have achieved varying degrees of success in practical applications. For example, a Gaussian mixture regression (GMR) model was proposed to realize continuous tool wear prediction based on features extracted from cutting force signal [21].** Kothuru et al. provided a solution to detect the wear conditions of the gear milling cutter in the cutting of

workpiece materials with hardness variations using audible sound signals [3].

The research above solved the tool wear problem by traditional modeling or machine learning under the constant working conditions. But the above method can't be used in multiple varieties, small batch production situation due to the frequent change of the tool working condition. Therefore, it is of great interest to solve the tool wear problem under variable conditions.

Zhang et al. developed the mapping time-variant model between tool wear and cutting parameters on difficult-to-machine materials. **For the first time, time is added as a factor of the experiment design in order to consider time variant [22],** but this is still an experimental attempt. Xie et al. found that the dimensionless cutting force time domain features are not sensitive to the change of cutting parameters, but sensitive only to change of the tool wear state [23]. Therefore, the tool wear state monitoring can be realized in variable parameter milling. Fan [24] uses a backpropagation artificial neural network to establish the mapping relationship between tool wear state and surface cutting temperature characteristic value and cutting condition parameters, so that the monitoring system can identify the tool state under variable cutting conditions and improve the flexibility of online monitoring of tool wear.

The methods above are to study tool wear under the condition of variable cutting parameters. All are based on the experimental method or the traditional modeling method; the flexibility of the application is poor; when other working conditions other than cutting parameters change, the model is not applicable; therefore, the tool wear under varying working conditions needs to be further studied.

2.2 Signal processing technology

In terms of indirect method tool wear feature extraction, how to accurately quantify the relationship between monitoring signals and the amount of wear is a difficulty in tool condition monitoring (TCM) [25]. The most common methods include Fourier transform and wavelet transform, time series analysis, etc. Wang et al. used the Fourier transform method to extract the frequency domain characteristics of the vibration signal and the acoustic emission signal. Combined with the statistical features of the time domain and the time-frequency domain features, a hidden Markov model is adopted to obtain the continuous wear value [26]. Lin et al. used wavelet transform to extract the energy of signals in different frequency bands as feature vectors. The relationship between the feature vector and tool wear was learned by a stacked auto-encoder network, and finally, the tool wear state prediction was realized. Alonso and Salgado used singular spectrum analysis (SSA) to extract information regarding flank wear from the measured sound signals [27]. Joseph et al. used empirical mode decomposition (EMD) to decompose the multi-component sound signal into

multiple intrinsic mode functions. The instantaneous frequencies with time and their amplitudes were obtained by applying Hilbert transform on each intrinsic mode function (IMF), so that cutting tool flank wear prediction is possible using emitted sound by Hilbert-Huang Transform (HHT) [28].

In fact, Fourier transform and the wavelet transform can only deal with linear non-stationary signals and are not adaptive. Since the monitoring signal is usually nonlinear and non-stationary, HHT is based on local features of the signal and can be decomposed adaptively. It is especially suitable for analyzing nonlinear non-stationary signals and therefore has a better application prospect.

2.3 LSTM network applications

LSTM is a variant network structure of RNN. It has unique advantages in the long-term memory of information and is therefore particularly suitable for dealing with time series problems. Wang et al. used the LSTM network to predict the fault time series based on the historical fault data of complex systems [29]. It verified that the established LSTM prediction model has strong applicability and higher accuracy in fault time series analysis. Ren et al. proposed a Chinese word segmentation method based on a LSTM network [30]. The results show that the LSTM network model-based method can obtain better performance than traditional machine learning methods. Wang et al. proposed a dynamic prediction method for tool life based on online learning [31]. Using the LSTM network as a model, the online learning module is integrated to enable the model to automatically update parameters during the machining process to achieve accurate prediction of tool life. Ma et al. propose a novel architecture of neural networks, LSTM NN, to capture nonlinear traffic dynamic in an effective manner [32]. Adlen et al. use the deep-length long-term memory network to deal with the advantages of time series and uses the stator currents of a three-induction induction motor captured in a steady state to realize real-time safety monitoring of the induction motor [33].

The update inside the LSTM network will be determined based on whether the state at the previous moment is memorized and by the input at the current time. Due to its unique "memory" advantage, LSTM networks are becoming more widely used in various fields.

3 Principle explanation

The tool remaining useful life prediction method we propose is based on the LSTM network. The schematic diagram is shown in Fig. 1.

This method is proposed for the same type of tool. First, we establish a unified representation of the working conditions according to the factors affecting the tool wear and then

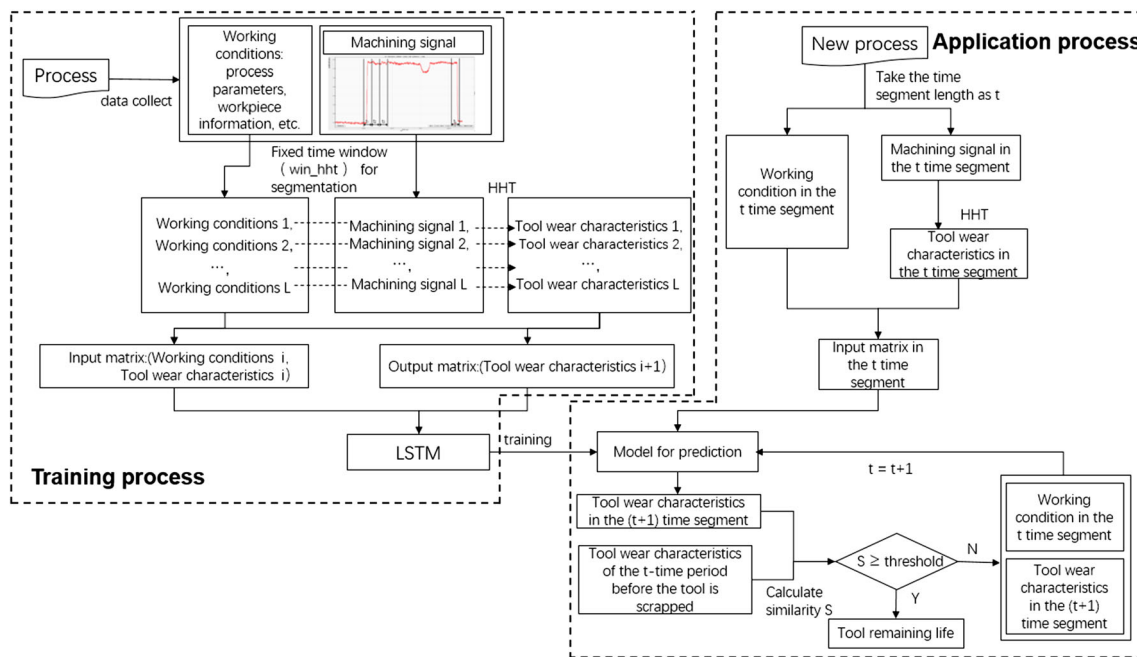


Fig. 1 Schematic diagram of the tool remaining useful life prediction method

extract the wear characteristics from the machining signal. The extracted wear characteristics and corresponding working conditions are combined with an input matrix to capture the complex spatiotemporal relationships under variable working conditions and lay a foundation for the subsequent prediction model. Finally, we use the LSTM network to learn the mapping relationship between the working scenes and the wear feature labels under variable conditions. The whole process can be divided into two stages: the training process and the application process.

(1) Training process

Collect the data of the whole life cycle processing process of the tool as the historical data to train the model, and set the total processing time length to D .

Step 1: The data collected during the processing is divided into working condition factors and D processing signals, such as working condition factors including process parameters and workpiece information. The machining signal is a torque signal.

Step 2: The time window length is fixed to win_hht , and the working condition and machining signal are divided into a number L of data segments in time series.

Step 3: The HHT is applied to each segment of the machining signal T_i to extract the tool wear characteristics of the segment F_i .

Step 4: The working condition segment Con_i and corresponding tool wear feature F_i are used as input, and the

tool wear feature F_{i+1} of the next time segment is used as output to train the LSTM network.

(2) Application process

Step 1: Taking the working condition segment Con_t and the machining signal segment T_t in the new process with a time segment length of t , the machining signal segment T_t is processed using the HHT to obtain the tool wear feature F_t for the t time segment.

Step 2: By inputting the working condition segment Con_t and corresponding tool wear feature F_t into the trained LSTM network, the tool wear feature F_{t+1} of the next time segment $t+1$ can be predicted.

Step 3: Calculate the similarity S between F_{t+1} and the tool wear characteristics of the t -time period before the tool is scrapped, if $S \geq threshold$, determine the tool remaining life to be 0. if $S < threshold$, the predicted tool wear characteristic F_{t+1} and the current working condition Con_t are taken as the next input matrix, and the process is repeated until the similarity reaches the set threshold. At this time, the tool remaining life is calculated according to the number of iterations.

3.1 Working condition information

In the actual machining process, there are many factors affecting the tool wear, such as workpieces, machine tools, and process parameters, which makes the tool wear prediction

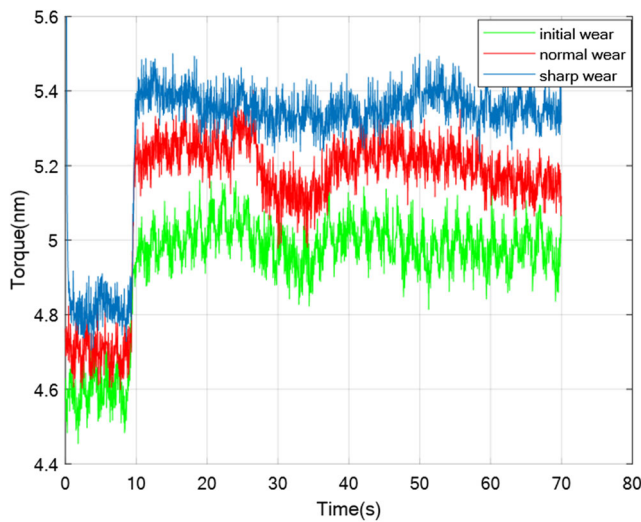


Fig. 2 Schematic diagram of the relationship between the torque signal and the tool wear

process extremely complicated. Therefore, we represent the working condition factors under variable working conditions in the form of working condition vectors, which are divided into four sub-vectors of process parameter, workpiece information. Then, the working condition vector Con can be expressed as:

$$Con = (P, W) \quad (1)$$

(1). Process parameter sub-conditions

Tool machining under different process parameters will result in different machining effects and have direct impact on tool wear. The main process parameters in the cutting process mainly include cutting speed (spindle speed), depth of cut, and feed rate. The process parameter sub-vector P is expressed as:

$$P = (n, \Delta x, \Delta y, \Delta z, f) \quad (2)$$

where n represents the spindle speed, f represents the feed rate and Δx , Δy and Δz represent the x , y and z coordinate difference of the adjacent time respectively.

(2). Workpiece information sub-conditions

The workpiece's material properties strength, hardness and thermal conductivity affect the cutting temperature, which in turn affects the tool wear. The influence of factors such as the clamping strength of the workpiece rigidity factor on the tool wear during machining is also prominent. Workpiece information sub-vector W is expressed as:

$$W = (K, \mu_s, E, R_m, \tau, HRA, e, Ak, C) \quad (3)$$

where K represents the thermal conductivity, μ_s represents the friction coefficient, E represents the positive elastic modulus, R_m represents the tensile strength, τ represents the shear strength, HRA represents Rockwell hardness, e represents elongation, Ak represents impact toughness, and C represents clamping strength.

3.2 Tool wear feature extraction

The process monitoring signal can reflect the tool wear after the actual machining starts, tool wear prediction model needs to distinguish the degree of tool wear, which means to obtain the wear label for the data set. Since the real monitoring signal is often nonlinear and non-stationary, the HHT is based on local features of the signal and can be adaptively decomposed, so it is especially suitable for analyzing nonlinear non-stationary signals. Therefore, we use the HHT to obtain the characteristics of the tool wear.

The process monitoring signal can reflect the tool wear after the actual machining starts. Common signals include

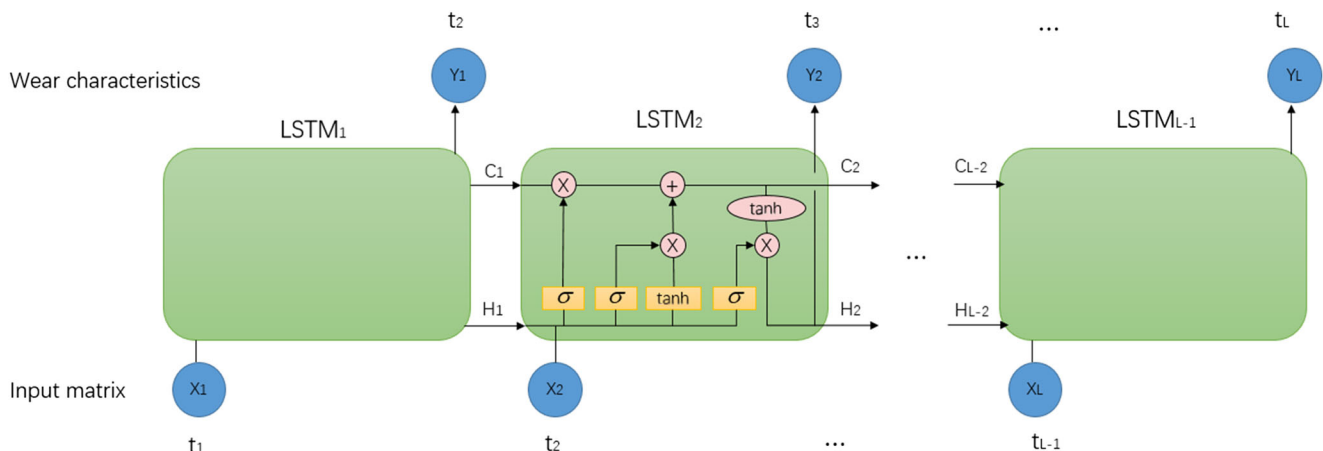


Fig. 3 Tool wear prediction LSTM model structure

Table 1 Experimental equipment

Equipment	Items
Machine tool	DMG125H Machine left
CNC system	Siemens 840D
Modular boring tool shank	21A.JT50.50-60
Boring tool blade	CCMT060204-EMF
Blank	QT500-7GB/T1348-1988
KOMET dynamic data acquisition system	Sampling frequency: 20 Hz

cutting force, vibration, acoustic emission (AE), torque signal and so on. Among them, the torque signal has lower sensitivity to tool wear than the cutting force signal, but has the advantages of low cost, convenient installation and measurement, and does not affect normal processing. In this paper, the torque signal is used as the process monitoring signal, and the relationship between the torque signal and the tool wear is shown in Fig. 2. It can be seen from the figure that under the same processing conditions, the torque is different in different wear stages. Therefore, the torque signal can be used as a process monitoring signal for tool wear.

Each IMF obtained by the EMD of the torque signal has a corresponding physical meaning. The studies in [28, 34] proved the sensitivity of the processing signal IMF amplitude and HHT marginal spectrum for the tool wear process. Therefore, this paper selects the amplitude average of the IMF decomposed by EMD and the larger amplitude point in the HHT edge spectrum as the wear characteristics.

Set the wear feature extraction window length win_hht , T represents the torque signal collected by the tool D during its entire life cycle $lifetime$ and the torque signal can be expressed as:

$$T = [T_1, T_2, \dots, T_L] \quad (4)$$

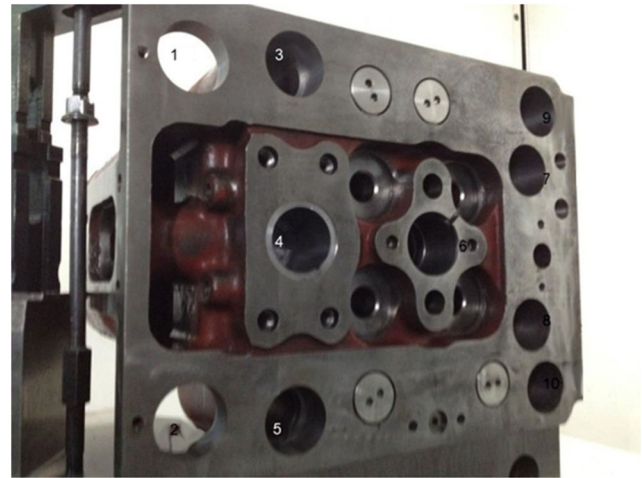
$$TL = \frac{lifetime}{win_hht} \quad (5)$$

where T_i represents the torque signal of the i -nd time segment, $i = 1, 2, \dots, L$

For each signal segmentation matrix T_i , first, T_i is decomposed into IMF by EMD, and then, the IMF component sensitive to wear variation is transformed by HHT to obtain an edge spectrum corresponding to the IMF component. The amplitude average A of the IMF, which is sensitive to tool

Table 2 Blade parameters

Blade model	Coating material	Tip radius (mm)	Front angle	Relief angle
CCMT060204-EMF	Titanium-nitride EB1220	0.4	6°	7°


Fig. 4 Blank

wear, and the maximum amplitude point I of the edge spectrum constitute the tool wear feature vector F . Wear feature item F_i can be obtained for each signal segmentation matrix T_i :

$$F_i = [A_i, I_i] \quad (6)$$

3.3 Construction of input matrix and output matrix

Set the time window length of the input data to win_con , set the initial time of this time window to m , and the input of the win_con network to X_m

$$X_m = \begin{bmatrix} Con_m & Con_{m+1} & \dots & Con_{m+win_con} \\ F_m & F_{m+1} & \dots & F_{m+win_con} \end{bmatrix} \quad (7)$$

where $Con_i (m \leq i \leq m + win_con)$ indicates the working condition factor corresponding to the i -th segment, and $F_i (m \leq i \leq m + win_con)$ is the wear characteristic corresponding to the i -th segment.

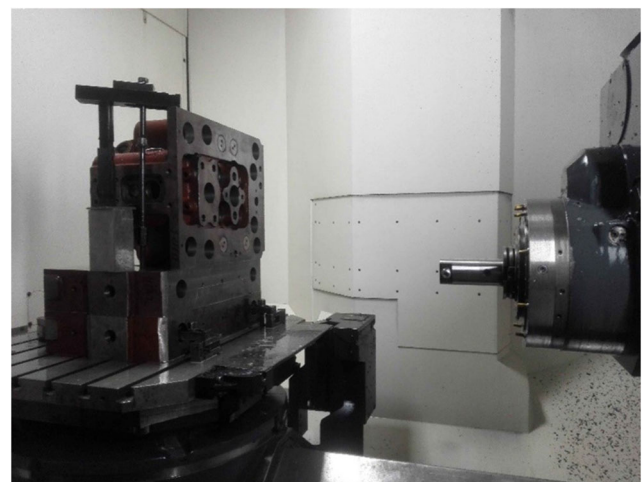

Fig. 5 Site processing device

Table 3 Experimental process parameters

Group number	Feed number	Rotating speed (r/min)	Feed rate (mm/min)	Cutting depth (mm)
TOOL1	35	600–960	70–96	0.25–0.60
TOOL2	40	700	40–260	0.25
TOOL3	30	800–1300	100	0.25
TOOL4	28	1000	100	0.10–0.90

Owing to wear characteristics obtained under the variable working conditions based on the indirect method have

working condition correlation, wear characteristics can be used to measure tool wear in working scenes. When the initial time of time window win_con is m , the output of the network is wear feature Y_m :

$$Y_m = [F_{m+1} \ F_{m+2} \ \dots \ F_{(m+1)+win_con}] \quad (8)$$

3.4 LSTM model and training

Variable working conditions have a complex space-time relationship. In space, the relationship between different working

Table 4 Data collection table

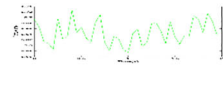
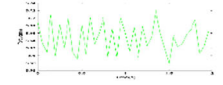
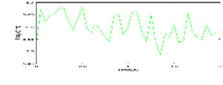
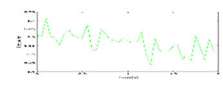
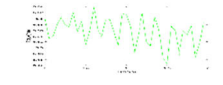
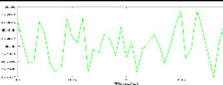
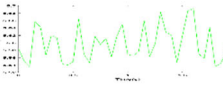
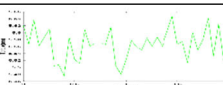
		Torque signal	Working conditions	Processing time (s)	Total processing time (s)
TOOL1	segment 1		rotating speed: 690r/min feed rate:69.3mm/min cutting depth:0.3mm	2	4
	segment 2		rotating speed: 693r/min feed rate:69mm/min cutting depth:0.3mm	2	
TOOL2	segment 1		rotating speed: 700r/min feed rate:182mm/min cutting depth:0.25mm	2	4
	segment 2		rotating speed: 700r/min feed rate:185mm/min cutting depth:0.25mm	2	
TOOL3	segment 1		rotating speed: 1049r/min feed rate:100mm/min cutting depth:0.25mm	2	4
	segment 2		rotating speed: 1056r/min feed rate:100mm/min cutting depth:0.25mm	2	
TOOL4	segment 1		rotating speed: 1000r/min feed rate:100mm/min cutting depth:0.25mm	2	4
	segment 2		rotating speed: 1000r/min feed rate:100mm/min cutting depth:0.3mm	2	

Table 5 Working condition of sample 5

Experiment number	Rotating speed (r/min)	Feed rate (mm/min)	Δx (mm)	Δy (mm)	Δz (mm)
1	690	80	0	0	–
2	693	80	0.001	0	0
400	714	80	–	0	–
			0.0–01		0.0–038

conditions and wear is complicated and difficult to analyze. Tool wear is not caused by a specific factor, but by the interaction of multiple factors in multiple processes. We use LSTM for high-dimensional modeling, eliminating redundant working condition parameters and extracting appropriate working condition factors for feature learning. On the other hand, due to the correlation of the tool state in time, the future wear state is the cumulative result of the change of the previous wear characteristics and the operating conditions. Due to its special memory cell structure, LSTM can handle the temporal correlation of working conditions and wear characteristics.

In summary, LSTM model has unique advantages in solving problems with complex correlations and memory accumulation effects. Therefore, according to the changing characteristics between working conditions and wear under variable working conditions, the LSTM model is used to solve the remaining useful life prediction problem in this scenario. The tool remaining useful life prediction LSTM model structure is shown in Fig. 3.

Set up the LSTM network and set the length of its window to win_con . L is calculated by Eq.(5). The input of the model is X :

$$X = \{X_1, X_2, \dots, X_L\} \quad (9)$$

$$X_i = \begin{bmatrix} Con_i & Con_{i+1} & \dots & Con_{i+win_con} \\ F_i & F_{i+1} & \dots & F_{i+win_con} \end{bmatrix} Y \quad (10)$$

The corresponding theoretical output is :

$$Y = \{Y_1, Y_2, \dots, Y_L\} \quad (11)$$

$$Y_i = [F_{i+1} \quad F_{i+2} \quad \dots \quad F_{(i+1)+win_con}] \quad (12)$$

Then, input X into the LSTM hidden layer. As can be seen from Fig. 3, the hidden layer contains L LSTM cells connected in time before and after. The output through the hidden layer is P :

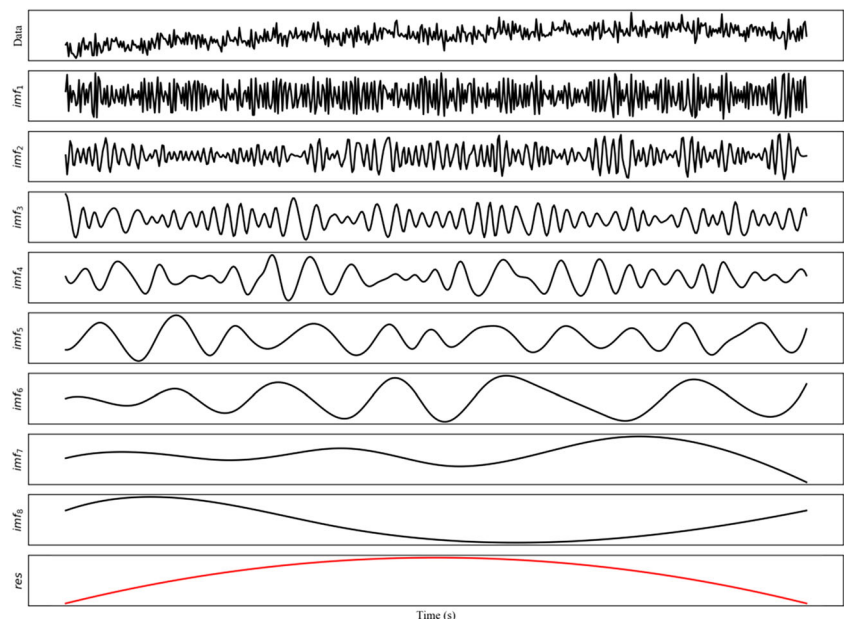
$$P = \{P_1, P_2, \dots, P_L\} \quad (13)$$

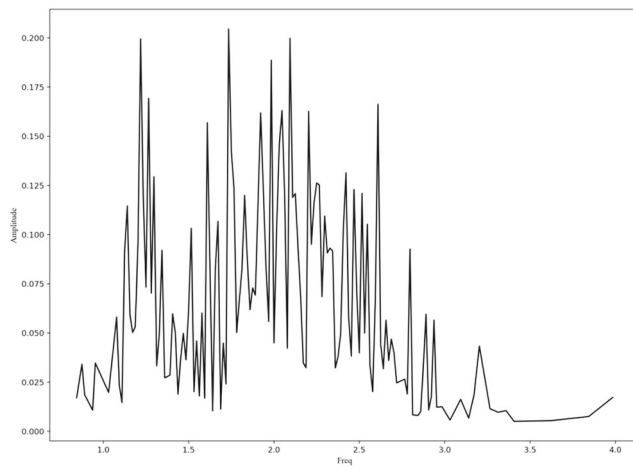
$$P_i = LSTM(X_i, C_{i-1}, H_{i-1}) \quad (14)$$

where C_{i-1} and H_{i-1} represent the state and output of the previous LSTM cell, respectively, and LSTM represents the forward propagation algorithm of the LSTM cell.

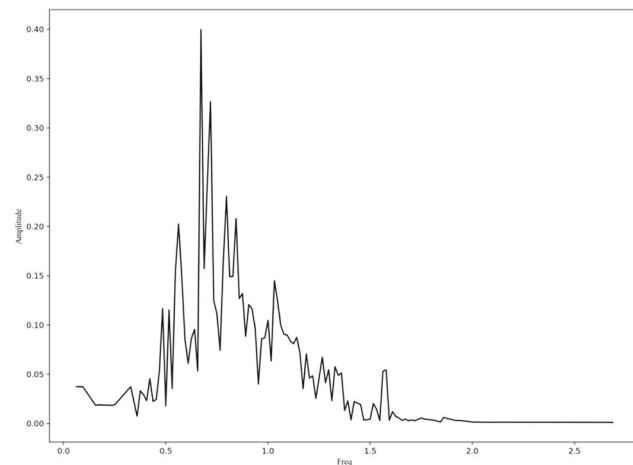
The mean square error (MSE) is selected as the error calculation formula, and the loss function of the training process can be defined as $loss$:

$$loss = \sum_{i=1}^L (P_i - Y_i)^2 / L \times win_con \quad (15)$$

Fig. 6 EMD decomposition of torque signal



(a) HHT marginal spectrum of IMF3



(b) HHT marginal spectrum of IMF4

Fig. 7 HHT marginal spectrum. **a** HHT marginal spectrum of IMF3. **b** HHT marginal spectrum of IMF4

Taking the minimum loss function as the optimization goal, given the random number of seeds, the initial learning rate and the number of training steps, the Adam optimization algorithm is used to continuously update the network weights, and finally, the LSTM hidden layer network is obtained.

3.5 Tool remaining useful life prediction

The judgment basis for the scrapping of the tool is as follows: when the tool flank wear reaches the blunt standard, the tool is considered to be scrapped.

Knowing the current operating condition segments Con_t and processing signal segments T_t , tool wear characteristics F_{t+1} of the next time segment are first predicted. Calculate the similarity S between F_{t+1} and the tool wear characteristics of the t -time period before the tool is scrapped, if $S \geq threshold$, determine the tool remaining life to be 0. if $S < threshold$, the predicted tool wear characteristic F_{t+1} and the current working condition Con_t are

taken as the next input matrix, and the process is repeated until the similarity reaches the set threshold. At this time, The number of iterations is l , and the remaining tool life is RL :

$$RL = l \times win_hht \times win_con \quad (16)$$

where $win_hht(win_hht = t)$ is the length of the time segmentation window of the machining signal, and win_con is the length of the window of the LSTM network.

4 Experimental setup

Due to the limitations of experimental equipment conditions and cost, the experiments under variable working conditions of this paper only collect part of the working condition data under different cutting parameters and do not cover workpiece material change data. However, this does not affect the logic of the method and the deduction of the model. The experimental equipment and materials are shown in Table 1.

The detailed parameters of the blade are shown in Table 2.

The blank used in the experiment is shown in Fig. 4. The hole depths of No. 4, No. 7, No. 8, No. 9, and No. 10 are 80 mm, and the diameter of the bottom hole is 57.55 mm. No. 3 and No. 5 holes have a depth of 40 mm and a bottom hole diameter of 57.55 mm. The No. 1 and No. 2 holes have a depth of 31 mm and the bottom hole has a diameter of 57.55 mm. The on-site processing equipment is shown in Fig. 5.

A total of four sets of blade life experiments were performed in the experiment. The process parameters are shown in Table 3.

5 Results and discussion

After the experiment, the working condition data files collected by the KOMET system are imported into the MySQL database. Each tool selects two working condition segments to display the collected data. The results are shown in Table 4.

For experiment 1, the machining time of TOOL1 is 128 min and the time is divided into 20 s, so that 384 torque signal segments and corresponding working condition segments are obtained. Each segment is used as a training sample.

Table 6 The top three large values of the HHT marginal spectrum

Experiment number	IMF number	1st amplitude value	2nd amplitude value	3rd amplitude value
1	3	0.203	0.199	0.163
	4	0.399	0.326	0.243

The fifth sample is taken as an example to illustrate the construction of the model input.

(1) Working condition of sample 5

Working conditions include: Rotating speed; Feed rate; Δx ; Δy ; Δz ; specific parameters are shown in Table 5:

(2) Torque signal feature extraction of sample 5

The tool wear characteristics are extracted from the torque signal of sample 5. The extracted terms are the IMF amplitude average and the top three large values of the HHT marginal spectrum. In Fig. 6, eight IMF maps are obtained by

decomposing the torque signal segments by EMD. Among them, IMF3 and IMF4 are sensitive to tool wear. Therefore, Hilbert marginal spectrum analysis is performed on IMF3 and IMF4. The analysis results are shown in Fig. 7:

As can be seen from Fig. 6, the amplitude average of IMF3 in sample 5 of TOOL1 is 8.4×10^{-5} , and the amplitude average of IMF4 is 1.4×10^{-4} . The first three large amplitudes of the corresponding HHT edge spectrum are shown in Table 6.

The input matrix $x_{400 \times 13}$ constructed by sample 5 is:

$$x_{400 \times 13} = \begin{bmatrix} 690 & 80 & 0 & 0 & -0.0033 & 8.4 \times 10^{-5} & 1.4 \times 10^{-4} & 0.203 & 0.199 & 0.163 & 0.399 & 0.326 & 0.243 \\ 693 & 80 & 0.001 & 0 & 0 & 8.4 \times 10^{-5} & 1.4 \times 10^{-4} & 0.203 & 0.199 & 0.163 & 0.399 & 0.326 & 0.243 \\ \dots & \dots & \dots & \dots & \dots & \dots & \dots & \dots & \dots & \dots & \dots & \dots & \dots \\ 714 & 80 & -0.001 & 0 & -0.0038 & 8.4 \times 10^{-5} & 1.4 \times 10^{-4} & 0.203 & 0.199 & 0.163 & 0.399 & 0.326 & 0.243 \end{bmatrix}$$

In this paper, the accuracy of the prediction model is verified by cross-validation method. Three groups of four experiments are used as the training set, and one group is used as the test set. The cross-validation scheme is shown in Table 7.

The tool remaining useful life prediction model uses a LSTM model. The number of hidden layer nodes is 64. The model uses the Adam optimization method for the training model; the batch size is 5; the loss function is the MSE.

Taking the No. 1 verification scheme as an example, that is, the data samples of TOOL1, TOOL2, and TOOL3 are used as training sets, and the data samples of TOOL4 are used as test sets. The curve of the MSE value changing with the number of training epochs during the training is shown in Fig. 8. The number of training epochs is 3,500. Although the loss function curve is noisy during training, this is due to poor data quality, but it eventually converges to 0.01367.

Table 7 The cross-validation scheme

Serial number	Training set	Test set
1	TOOL1	TOOL4
	TOOL2	
	TOOL3	
2	TOOL1	TOOL3
	TOOL2	
	TOOL4	
3	TOOL1	TOOL2
	TOOL3	
	TOOL4	
4	TOOL2	TOOL1
	TOOL3	
	TOOL4	

The above processes are repeated for the verification schemes No. 2, No. 3, and No. 4, and the MSE value curves of the tool remaining useful life prediction model are shown in Fig. 9a, b, and c.

It can be seen from Fig. 9 that the loss function of the second, third and fourth verification schemes converge after training the LSTM network for a certain number of epochs. The MSE values are 0.00954; 0.01298; 0.01673, respectively.

When the LSTM network training is completed, the test set data is put into the trained LSTM network and the predicted result and the actual result are yielded as shown in Table 9.

For regression prediction problems, we use R -squared to evaluate the model as follows.

$$R^2 = 1 - \frac{\sum (y - \hat{y})^2}{\sum (y - \bar{y})^2} \quad (17)$$

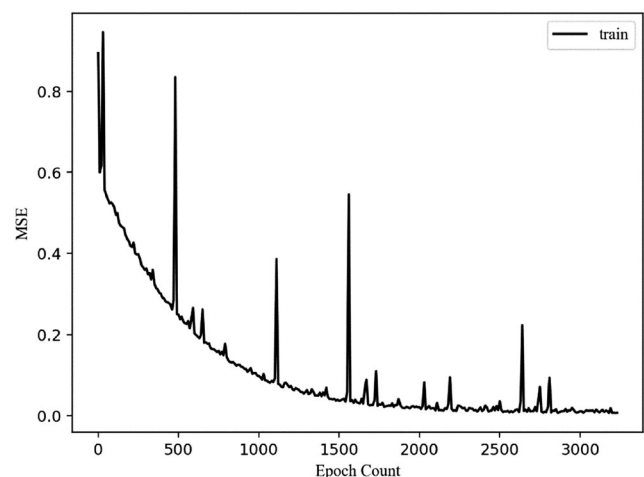
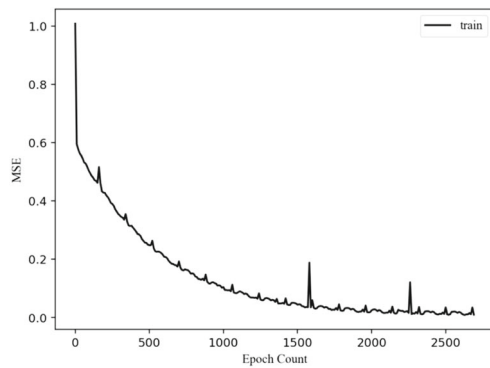
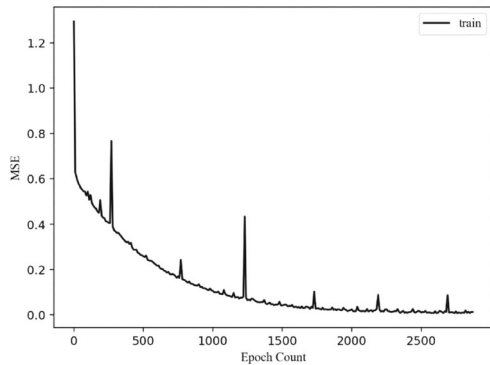


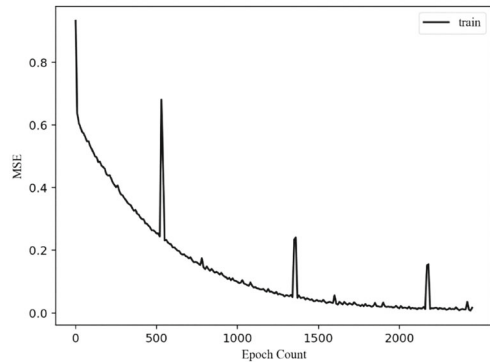
Fig. 8 the MSE value curve of No. 1 verification scheme



(a) the MSE value curve of No. 2 verification scheme



(b) the MSE value curve of No. 3 verification scheme



(c) the MSE value curve of No. 4 verification scheme

Fig. 9 The MSE value curves of the tool remaining useful life prediction model. **a** The MSE value curve of No. 2 verification scheme. **b** The MSE value curve of No. 3 verification scheme. **c** The MSE value curve of No. 4 verification scheme

The numerator represents the sum of the squared difference between the true value and the predicted value. The denominator represents the sum of the squared differences between the true value and its mean. The closer the result is to 1, the

Table 8 Comparison of predicted and actual values (No. 1 verification scheme)

Serial number	Actual value (min)	Predicted value (min)
1	52	40
2	37	28
3	22	20

Table 9 Comparison of predicted and actual values on test points

Verification scheme number	Serial number	Actual value (min)	Predicted value (min)
2	1	44	40
	2	29	28
	3	14	14
3	1	48	40
	2	33	32
	3	18	18
4	1	48	38
	2	33	34
	3	18	16

closer the predicted value is to the true value, i.e. the better the model fits. Therefore, the R^2 -squared evaluation of the test points in this paper is obtained as $R^2 = 0.7806$.

From Figs. 8 and 9, it can be seen that the model training process has a good fitting effect. It can converge faster in the training period and is finally at a lower level. At the same time, from the prediction results in Table 8 and Table 9 we know that there is a certain mismatch between the predicted and the true amount of remaining life time. In general, however, tool remaining useful life prediction under variable working conditions can be achieved.

6 Conclusion

In this paper, we propose a method for predicting tool remaining useful life under variable working conditions based on the LSTM network. First, we establish a unified representation of the working conditions according to the factors affecting the tool wear. Then, we extract the wear characteristics from the process monitoring signal. The extracted wear characteristics and other working conditions are constructed into a matrix to capture the complex spatiotemporal relationships under variable working conditions. Owing to the unique advantages of the LSTM model in solving problems with complex correlations and memory accumulation effects, we establish the tool remaining useful life prediction model under variable working conditions. Finally, the experiment illustrates the effectiveness of the proposed method. However, due to experimental conditions and other limitations, the quality of experimental data may have some adverse effects on the accuracy of prediction. Future work will focus on more in-depth exploration of the various stages of the approach to optimize the accuracy of the forecast.

Funding information The work is financially supported by the National Defense Basic Scientific Research program of China through approval no. JSCG2016205B006 and the National Science and Technology Major Project of China through approval no. 2012ZX04011041.

References

1. Attanasio A, Ceretti E, Giardini C (2013) Analytical models for tool wear prediction during AISI 1045 turning operations. *Procedia Cirp* 8(11):218–223
2. Ji W, Shi J, Liu X, Wang L, Liang SY (2017) A novel approach of tool wear evaluation. *J Manuf Sci Eng* 139(9):091015
3. Kothuru A, Nooka SP, Victoria PI & Liu R. 2017 “Application of audible sound signals for tool wear monitoring and workpiece hardness identification in gear milling using machine learning techniques.” ASME 2017 International Design Engineering Technical Conferences and Computers and Information in Engineering Conference, Volume 10.
4. Mikolajczyk T, Nowicki K, Klodowski A, Pimenov YD (2017) Neural network approach for automatic image analysis of cutting edge wear. *Mech Syst Signal Process* 88:100–110
5. Kurada S, Bradley C (1997) A review of machine vision sensors for tool condition monitoring. *Comput Ind* 34(1):55–72
6. Zhang C, Zhang J (2013) On-line tool wear measurement for ball-end milling cutter based on machine vision. *Comput Ind* 64(6):708–719
7. Nan X, Duan M, Gao Y, Zheng P (2017) Tool wear prediction approach based on power sensor. *J Tongji Univ* 453:420–426
8. Hochreiter S, Schmidhuber J (1997) Long short-term memory. *Neural Comput* 9(8):1735–1780
9. Graves A (2013). “Generating sequences with recurrent neural networks.” *Computer Science*
10. Munozescalona P, Diaz N, Cassier Z (2011) Prediction of tool wear mechanisms in face milling AISI 1045 steel. *J Mater Eng Perform* 21(6):797–808
11. Chincharikar S, Choudhury SK (2015) Predictive modeling for flank wear progression of coated carbide tool in turning hardened steel under practical machining conditions. *Int J Adv Manuf Technol* 76:1185–1201
12. Yang S, Zhu G, Xu J, Fu Y (2013) Tool wear prediction of machining hydrogenated titanium alloy Ti6Al4V with uncoated carbide tools. *Int J Adv Manuf Technol* 68(1):673–682
13. Cheon S, Kim N (2016) Prediction of tool wear in the blanking process using updated geometry. *Wear* 352–353:160–170
14. Braglia M, Castellano D (2014) Diffusion theory applied to tool-life stochastic modeling under a progressive wear process. *J Manuf Sci Eng-Trans Asme* 136(3):031010
15. Braglia M, Castellano D (2015) Improving tool-life stochastic control through a tool-life model based on diffusion theory. *J Manuf Sci Eng-Trans Asme* 137:4
16. Karuppusamy NS, Pal Pandian P, Lee H-S and Kang B-Y. (2015) “Tool wear and tool life estimation based on linear regression learning.” international conference on mechatronics and automation 17–21.
17. Daddona D, Ullah AM, Matarazzo D (2017) Tool-wear prediction and pattern-recognition using artificial neural network and DNA-based computing. *J Intell Manuf* 28(6):1285–1301
18. Rangwala S, Dornfeld D (1990) Sensor integration using neural networks for intelligent tool condition monitoring. *J Eng Indu* 112(3):219
19. Byrne G, Dornfeld D, Inasaki I, Ketteler G, König W, Trti R (1995) Tool Condition Monitoring (TCM) — The Status of Research and Industrial Application. *CIRP Ann* 44(2):541–567
20. Wilcox SJ, Reuben RL, Souquet P (1997) The use of cutting force and acoustic emission signals for the monitoring of tool insert geometry during rough face milling. *Int J Mach Tool Manu* 37(4):481–494
21. Wang G, Qian L, Guo Z (2013) Continuous tool wear prediction based on Gaussian mixture regression model. *Int J Adv Manuf Technol* 66(9):1921–1929
22. Zhang, Peipei, and Y. Guo. (2016) Mapping time-variant modelling of tool wears and cutting parameters on difficult-to-machine materials. *Proceedings of the 10th World Congress on Engineering Asset Management (WCEAM 2015)*. Springer International Publishing.
23. Qinglu X, and Guofeng W. (2016) “Changed parameters of milling tool wearing condition monitoring research.” *J Mech Sci Technol* (12):1842–1847.
24. Wei F. (2008) “Research on tool state identification based on infrared temperature measurement.” Shanghai jiaotong University.
25. Yu J, Liang S, Tang D, Liu H (2016) A weighted hidden Markov model approach for continuous-state tool wear monitoring and tool life prediction. *Int J Adv Manuf Technol* 91(1–4):1–11
26. Xiaoqiang W, Zhang Yun, Huamin Z, and Yang F. (2016) “Tool wear continuous monitoring based on hidden Markov model.” *Mod Mach Tool Autom Proc Technol*, (10):87–90.
27. Alonso FJ, Salgado DR (2005) Application of singular spectrum analysis to tool wear detection using sound signals. *Proc Instit Mech Eng Part B: J Eng Manuf* 219(9):703–710
28. Emerson Raja J, Kiong LC, and Soong LW (2011) “Emitted sound amplitude analysis using Hilbert Huang Transformation for cutting tool flank wear prediction.” *International Conference on Computing & Communication Systems Springer, Berlin, Heidelberg*.
29. Xin W, Ji W, Chao L, Haiyan Y, Yanli D, and Wensheng N. (2018) “Fault time series prediction based on LSTM recurrent neural network.” *J Beijing Univ Aeronaut Astronaut*, (4):772–784.
30. Zhihui R, Haoyu X, Songlin F, Han Z, Jun S (2017) Sequence marking Chinese word segmentation based on LSTM network. *Comp Appl Res* 34(5):1321–1324
31. Qiang W, Yingguang L, Xiaozhong H, Changqing L, Haiji C (2019) Dynamic prediction method of nc machining tool life based on online learning. *Aerospace Manuf Technol* 62(07):49–53
32. Ma XL, Tao ZM, Wang YH, Yu HY, Wang YP (2015) Long short-term memory neural network for traffic speed prediction using remote microwave sensor data. *Trans Res Part C: Emerg Technol* 54:187–197
33. Adlen K, Abderrezak M, Ridha K, Batouche M (2018) Real-time safety monitoring in the induction motor using deep hierarchic long short-term memory. *Int J Adv Manuf Technol* 99(9–12):2245–2255
34. Huibin S, Weilong N, Junyang W (2015) Tool wear feature extraction based on Hilbert-Huang Transform. *J Vib Shock* 34(4):158–164

Publisher's note Springer Nature remains neutral with regard to jurisdictional claims in published maps and institutional affiliations.